

RESEARCH ARTICLE

Improvement of sticking in tablet compaction for tocopherol acetate

Yukoh Sakata and Hiroyuki Yamaguchi

Healthcare Research Institute, Wakunaga Pharmaceutical Co., Ltd.

Abstract

We have found that the addition of xylitol solution effectively improves the sticking observed in tablet compaction using a powder prescription including kneading mixtures comprising tocopherol acetate (TA)/Florite® RE (FLR) blends. The aim of the present study was to investigate the distribution states of TA and xylitol in kneaded mixtures comprising TA/FLR/xylitol blends and the particle states of these mixtures in order to derive an appropriate powder formulation for tablet compaction. Nitrogen gas adsorption analysis revealed that xylitol is distributed on the interparticle and intraparticle pores of FLR in the same manner as TA. Moreover, it was found that xylitol was distributed in an incomplete crystalline form because of its interaction with FLR particles in the kneaded mixtures comprising TA/FLR/xylitol blends. It was also observed that the surfaces of the particles of the kneaded mixtures comprising TA/FLR blends changed from rough to smooth because of kneading with xylitol. The occurrence of sticking can be prevented not only by the addition of xylitol but also by changing the particle states of TA/FLR/xylitol blends.

Keywords: Tocopherol acetate, Florite® RE, xylitol, sticking, interaction

Introduction

Oily medicines dissolved in oleic acid as an oil have generally been manufactured and marketed commercially in a soft capsule form¹. Making a solid preparation of an oily medicine is expected to improve the compliance and utility of the medicine for patients^{2,3}. From the viewpoint of the final dosage form of solid dispersion particles, the use of a tablet is desirable among the various types of dosage forms⁴. A common problem encountered during tablet compaction is sticking, which occurs when particles of the tablet formulation consisting of the oily medicine and excipients adhere to the punch face. These problems can hinder the production of high-quality tablets. In addition, various factors related to the machinery and the environment, such as the surface condition of the punch, compression force and speed, and temperature and humidity around the machine, may also have an effect. Schmidt et al.⁵ measured the force required to remove the tablet from the punch surface. Naito et al.^{6–8} reported a means of measuring the slipping force of a tablet surface and the passive pressure of the lower punch during compression.

Toyoshima et al.⁹ studied the relationship between sticking and the tablet surface roughness. Factors related to the materials used, that is, melting point, wettability, size and distribution, surface condition, and hardness of particles, may be responsible for sticking. Danjo et al.¹⁰ reported the effects of water content on sticking during compression, because sticking occurs easily with an increase in the water content.

Previous publications have reported the use of porous materials as a carrier to disperse the drug molecules in the pores^{11,12}. Examples of porous carriers that have been used for pharmaceutical purposes include porous silicon dioxide (Sylysia), magnesium aluminometasilicate (Neusilin), and porous calcium silicate (Florite® RE [FLR]).

Takeuchi et al. reported that solid dispersion particles prepared using fine porous silica (Sylysia 350) as a carrier by the spray-drying method can improve the dissolution property of poorly water-soluble drugs^{13,14}. Gupta et al.¹⁵ reported that the amorphous Neusilin-bound states of four drugs, namely, ketoprofen, indomethacin,

Address for Correspondence: Yukoh Sakata, Healthcare Research Institute, Wakunaga Pharmaceutical Co., Ltd., 1624 Shimokotachi, Kodacho, Akitakatashi, Hiroshima 739-1195, Japan. Tel: +81-826-45-2331. Fax: +81-826-45-4351. E-mail: sakata_y@wakunaga.co.jp

(Received 10 September 2010; revised 21 January 2011; accepted 26 January 2011)

naproxen, and progesterone, were physically stable during storage. Carriers include porous carriers, which are low-density solids with an open- and closed-pore structure that provide a large exposed surface area for drug loading. Owing to their wide range of useful properties, porous carriers have been used for many pharmaceutical purposes including the development of novel drug delivery systems such as floating drug delivery systems and sustained drug delivery systems, improvement of the solubility of poorly soluble drugs, and enzyme immobilization¹⁶⁻²¹. Therefore, porous materials were used as a carrier to disperse the drug molecules in the pores^{11,12}.

FLR is a porous calcium silicate $[2\text{CaO} \cdot 3\text{SiO}_2 \cdot m\text{SiO}_2 \cdot n\text{H}_2\text{O} \ (1 < m < 2, 2 < n < 3)]$ that possesses many interparticle and intraparticle pores, particularly of sizes 12 and 0.15 μm , respectively, on its surface²¹, and its use has been approved as a medicinal additive. FLR has been used to adsorb oily and other drugs as a compressive agent in pharmaceuticals and to improve solubility²². Yuasa et al. reported that FLR exhibited an excellent liquid-holding ability as compared with other excipients²³. When a powder that adsorbed tocopherol acetate (TA) as an oily medicine was prepared using FLR as an adsorbing carrier form, problems such as sticking commonly occurred during tablet compaction. We have found that sticking due to a tablet formulation containing TA could possibly be improved by the addition of a xylitol solution. It is well-known that the occurrence of sticking depends on the characterization and surface condition of particles. The objective of the present study was to ascertain the distribution states of TA and xylitol on the FLR particles; this is basic information that will be required to devise the formulation and manufacturing process for a tablet containing an oily medicine.

Materials and methods

Materials

TA (MW=472.75; Eisai Co., Ltd., Tokyo, Japan) was used as a model drug. Porous calcium silicate (FLR; Eisai Co., Ltd.) was used as an adsorbing carrier for TA. Xylitol (MW=152.15) was purchased from Towa Chemical Industry Co., Ltd. (Osaka, Japan). Microcrystalline cellulose (Avicel PH101; Asahi Chemical Industries Co., Tokyo, Japan) and anhydrous dibasic calcium phosphate (Tomita Pharmaceutical Co., Ltd., Tokushima, Japan) were used as excipients. Magnesium stearate (Mg-St; Taihei Chemical Industries Co., Ltd., Osaka, Japan) was used as a lubricant and a glidant.

Preparation of TA tablets

TA solutions of 33.3% concentration were prepared by dissolving TA in ethanol, and this solution was added to FLR. Kneading mixtures of TA and FLR were prepared and then dried at 50°C for 3 h. After drying, the kneaded mixtures were passed through a 30-mesh (500 μm) sieve. Xylitol solutions of 50% concentration were prepared by dissolving xylitol in purified water, and this solution

was added to the kneaded mixtures comprising TA/FLR. Kneaded mixtures comprising TA/FLR and a xylitol solution of 50% (w/w) were prepared at a weight ratio of 11:5 and then dried at 50°C for 12 h; screened through a 30-mesh (500 μm) sieve; mixed with microcrystalline cellulose, anhydrous dibasic calcium phosphate, and magnesium stearate; and compressed into tablets at 500, 750, and 1000 kg/cm² by using 8-mm diameter round and shallow concave punches on a rotary tablet press (Kikusui Engineering, Kyoto, Japan).

Preparation of samples

Kneaded mixtures comprising TA/FLR were prepared at weight ratios of 0:100, 33:67, 50:50, and 55:45, and those comprising TA/FLR and xylitol (xylitol solutions of 50% concentration) were prepared at a weight ratio of 11:5. Nitrogen gas adsorption and attenuated total reflection Fourier transform infrared (ATR FT-IR) analyses were carried out on these mixtures to study the distribution states of TA and xylitol on FLR particles. Kneaded and physical mixtures comprising xylitol/FLR were prepared at weight ratios of 100:0, 75:25, 50:50, 30:70, and 0:100. Scanning electron microscopy (SEM), differential scanning calorimetry (DSC), powder X-ray diffraction (PXRD), and ATR FT-IR analyses were carried out on these mixtures to study the interaction between xylitol and FLR. Samples were prepared as kneaded and physical mixtures by grinding them to a fine powder (particle size <710 μm) in an agate mortar and pestle followed by drying at 50°C for 12 h.

Specific surface area and pore size distribution measurement

The specific surface area was measured by the air-permeability method using a specific surface area meter (Shimadzu Seisakusho Co., Ltd.; Type SS-100). Samples were heated at 50°C for 5 h under vacuum before measurement. The specific surface area was calculated according to the Brunauer-Emmett-Teller (BET) equation.

Surface observation of FLR particles

Samples were mounted onto aluminium stubs and gold coated in a sputter coater to a thickness of ~10 μm . The coated samples were then viewed at a magnification of 400 \times using a field emission SEM (FE-SEM; JEOL, Tokyo, Japan). The beam accelerator voltage was set to 25 kV and the current was set to 12 μA .

ATR FT-IR spectroscopy

Each sample powder was analyzed in an ATR FT-IR spectrometer (FT-IR-620; Jasco, Tokyo, Japan) equipped with a deuterated L-alanine triglycine sulfate (DLATGS) detector. The sample powder was placed in a horizontal ATR accessory (Pike Tech., Madison, WI) with a zinc selenide prism for the analysis. All spectra were carried out at 52 scans and a resolution of 4 cm⁻¹ at ambient temperature (25°C). Three batches of each sample powder were

analyzed. The individual spectrum of three analyses of each sample was obtained and averaged to produce a single spectrum for subsequent data processing. Spectral Manager for Windows software (Jasco) was used for data acquisition and holding.

DSC analysis

A thermal analysis of the samples was performed with a DSC (DSC EXSTRA 6000 with a DSC 30E measuring cell; Seiko, Chiba, Japan). Approximately 5 mg of a sample was weighed into the DSC pan, and the sealed pan was placed in the sample side of the instrument. An identical reference pan was placed in the reference side. Scans were carried out at a rate of 10°C/min at temperatures between 45°C and 120°C, using a nitrogen gas purge at 50 mL/min. The extrapolated onset temperature (T_m) was considered as the temperatures of the peaks.

PXRD analysis

PXRD analysis was carried out at room temperature with a type Rint2550VHF diffractometer (Rigaku, Tokyo, Japan). Measurement conditions were as follows: target, copper; filter, K_α ; voltage, 40 kV; current, 450 mA; time constant, 1 sec; step slit, 1.0°; counting time, 1.0 sec; measurement range, $2\theta = 10^\circ$ – 60° .

Results and discussion

Particle states of kneaded mixtures comprising TA/FLR/xylitol blends

Thus far, it is known that sticking occurs during tablet compaction when particles of a tablet formulation comprising an oily medicine and excipients adhere to the punch face. In general, porous carriers such as

porous silicon dioxide (Sylysia), FLR, magnesium aluminometasilicate (Neusilin), and porous ceramic can be used to powderize oily medicines²³. In order to design an appropriate tablet formulation consisting of an oily medicine and excipients, we selected FLR because it has excellent liquid-holding ability as compared with other excipients²³.

The formulae of the tablets (200 mg/tablet) containing TA are listed in Table 1. Sticking was observed in the case of the kneaded mixtures comprising TA/FLR blends (Figure 1A, Rp. 1 in Table 1). However, it was found that sticking could be reduced by adding a xylitol solution to the kneaded mixtures comprising TA/FLR blends (Figure 1B, Rp. 2 in Table 1). In particular, it was observed that sticking did not occur for weight ratios between 0:100 and 55:45 (TA:FLR) for kneaded mixtures comprising TA/FLR blends in the presence of xylitol (Rp. 2). The characteristics of TA tablets containing kneaded mixtures comprising TA/FLR blends, such as the actual size, tablet hardness, friability, and disintegration time, were significantly different from those of tablets containing kneaded mixtures comprising TA/FLR/xylitol blends (Table 2). The hardness and disintegration time of TA tablets containing kneaded mixtures comprising TA/FLR blends increased and decreased, respectively, by the addition of xylitol to the kneaded mixtures.

Various factors related to the materials used, that is, melting point, wettability, size and distribution, surface condition, and the hardness of the particles, may be responsible for sticking. The particle states of the kneaded mixtures comprising TA/FLR/xylitol blends and the effects of TA and xylitol on the BET surface area of FLR

Table 1. Tocopherol acetate (TA) tablet formulations (mg).

	Rp. 1	Rp. 2
Florite (FLR)	250	250
Tocopherol acetate (TA)	300	300
Xylitol	–	250
Microcrystalline cellulose	500	250
Anhydrous dibasic calcium phosphate	140	140
Magnesium stearate	10	10
Total (mg)	1200	1200

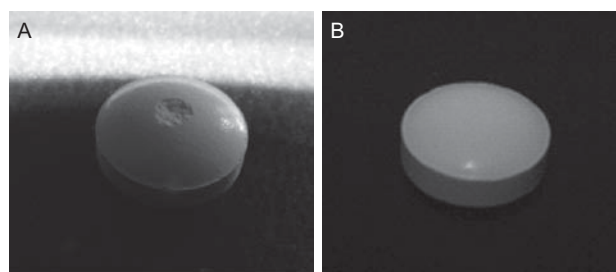


Figure 1. Photographs of the formulation of tablets containing kneaded mixtures comprising TA/FLR and TA/FLR/xylitol blends. Key: (A) TA/FLR and (B) TA/FLR/xylitol.

Table 2. Characteristics of tocopherol acetate (TA) tablets.

Rp	CF ^a (kg/cm ²)	T ^b (mm)	H ^c (mm ³ /g)	Friability (%)	DT ^d (min)
Rp. 1	500	4.90 ± 0.01	2.23 ± 0.07	0.239 ± 0.019	24.10 ± 0.50
	750	4.17 ± 0.01	3.86 ± 0.10	0.211 ± 0.023	26.30 ± 1.54
	1000	3.78 ± 0.02	5.22 ± 0.15	0.207 ± 0.014	28.59 ± 1.33
Rp. 2	500	5.03 ± 0.01	3.42 ± 0.09	0.025 ± 0.003	8.25 ± 0.88
	750	4.70 ± 0.01	4.51 ± 0.14	0.017 ± 0.001	8.50 ± 1.47
	1000	4.29 ± 0.01	6.69 ± 0.16	0.009 ± 0.002	8.80 ± 1.45

^aCompression force.

^bThickness.

^cTablet hardness.

^dDisintegration time.

particles were investigated using nitrogen gas adsorption analysis. Nitrogen gas adsorption is commonly used in the characterization of the properties of porous materials, such as specific surface area.

Figure 2(a) shows the effects of TA on the BET surface area of intact FLR. The BET surface area of intact FLR was found to be 135.7 m²/g. This was in agreement with the data for intact FLR particles from a previous study²⁴. The BET surface area of intact FLR decreased linearly with an increase in the TA weight ratio, with a correlation coefficient constant of 0.999.

Figure 2(b) shows the effects of xylitol (solution) on the BET surface area of the kneaded mixtures comprising TA/FLR blends. Kneaded mixtures consisting of TA/FLR blends and xylitol were prepared at a weight ratio of 11:5. The BET surface areas of the kneaded mixtures comprising TA/FLR blends were strongly decreased by the addition of xylitol, and the relationship was found to be inversely proportional with a correlation coefficient constant of 0.998. Yuasa et al. reported that FLR exhibited an excellent liquid-holding ability²³. Moreover, FLR possesses many interparticle and intraparticle pores²¹. The decrease in the BET surface area of FLR on addition of TA and the decrease in the surface area of TA/FLR blends on addition of xylitol, therefore, suggest that TA and xylitol may be distributed on the interparticle and intraparticle pores of FLR in kneaded mixtures comprising TA/FLR/xylitol blends.

SEM analysis was carried out to inspect the surface appearance of kneaded mixtures comprising TA/FLR and TA/FLR/xylitol blends (Figure 3). Figure 3A shows a SEM photograph of intact FLR. Intact FLR, which has an amorphous structure with flower-shaped particles (reported by Yuasa et al.²³), was strongly affected by kneading with TA (Figure 3B). Moreover, the surface appearance of the kneaded mixtures comprising TA/FLR blends was affected by kneading with xylitol (Figure 3C). The kneaded mixtures comprising TA/FLR blends exhibited a rough surface with many pores. In contrast, the kneaded mixtures comprising

TA/FLR/xylitol blends exhibited a smooth surface. It is well-known that the occurrence of sticking depends on the characteristics and surface condition of particles. Since sticking in a tablet formulation containing TA could possibly be reduced by the combination of FLR and a xylitol solution, the occurrence of sticking may be related to the particle states of the kneaded mixtures

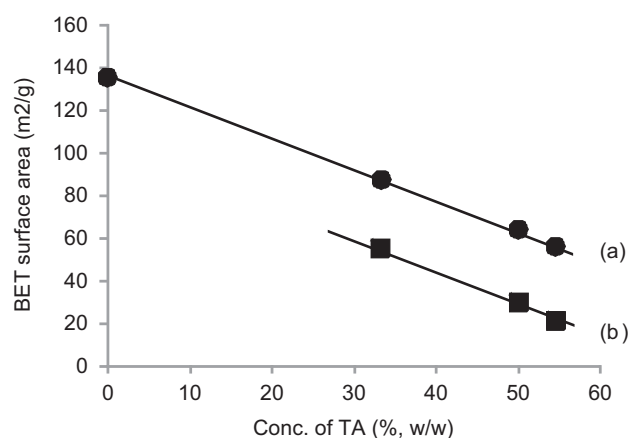


Figure 2. Effect of TA (a) and xylitol (b) on BET surface area of FLR particles and on kneaded mixtures comprising TA/FLR blends.

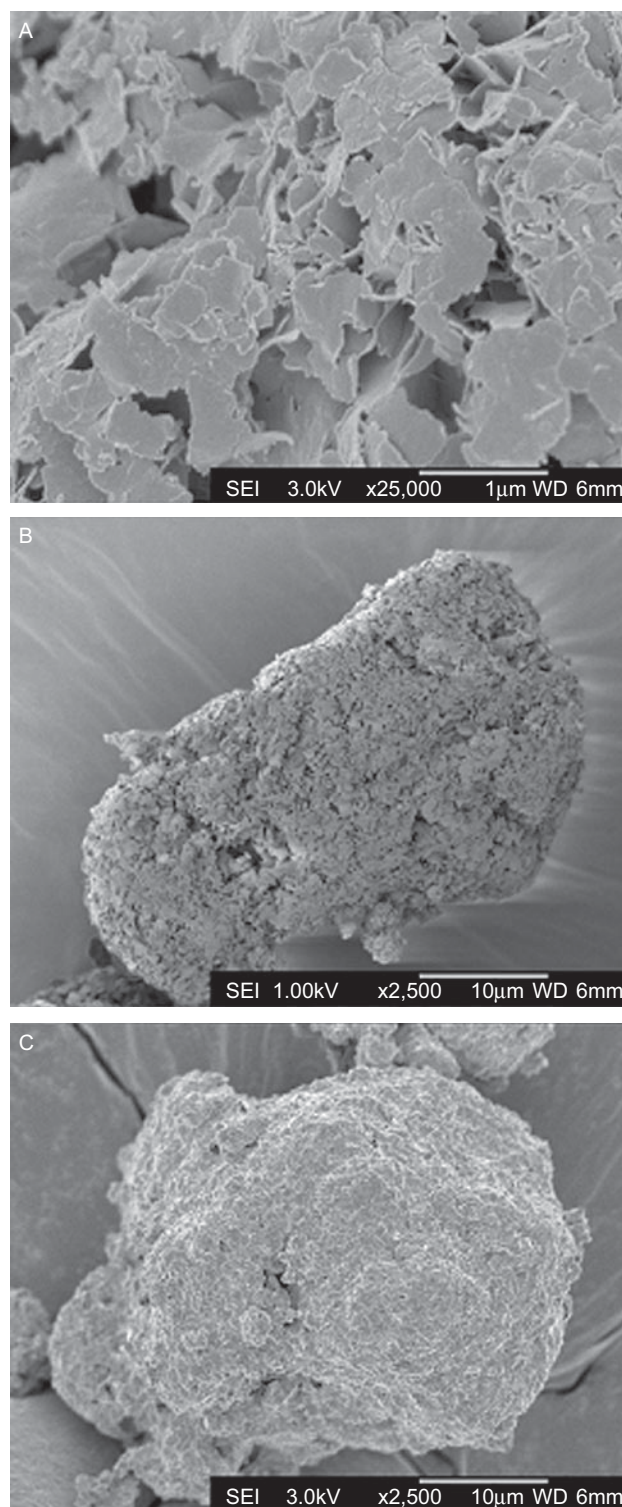


Figure 3. SEM observation of intact FLR(A) and of the kneaded mixtures comprising TA/FLR(B) and TA/FLR/xylitol(C) blends.

comprising TA/FLR/xylitol blends. In addition, as is shown in Figure 2, TA and xylitol are thought to be distributed on the interparticle and intraparticle pores of FLR in kneaded mixtures comprising TA/FLR/xylitol blends. Therefore, it is suggested that the particle states of the kneaded mixtures comprising TA/FLR/xylitol may be related to the distribution states of TA and xylitol on FLR particles.

Prediction of distribution states of TA and xylitol on the kneaded mixtures comprising TA/FLR/xylitol blends

FT-IR spectroscopy is a powerful tool that is widely used for the study of chemical and physical changes in the molecular structure of biological materials. Recently, the ATR FT-IR method has been used for the study of the

surface characterization of films and crystal powders^{25,26}. In this section, to confirm the distribution states of TA and xylitol on the particles comprising TA/FLR/xylitol blends, ATR FT-IR analysis was performed.

Figure 4 shows the FT-IR spectra of TA (Figure 4A), FLR (Figure 4B), kneaded mixture comprising TA and FLR at 50:50 (w/w) (Figure 4C), xylitol (Figure 4D), and kneaded mixture comprising TA, FLR, and xylitol at 50:50:30 (w/w/w) (Figure 4E). The FT-IR spectra of TA and the other samples were obtained by the transmittance and ATR methods, respectively. The peaks of TA are assigned as follows²⁷: 1210 cm⁻¹, C-O, -C=O, and -C-O- stretching; 1370 cm⁻¹ and 1464 cm⁻¹, CH vibration; 1760 cm⁻¹, C=O stretching. The representative IR bands of native TA (Figure 4A) were shifted slightly by the kneading of FLR powder. In the kneaded mixture comprising TA/

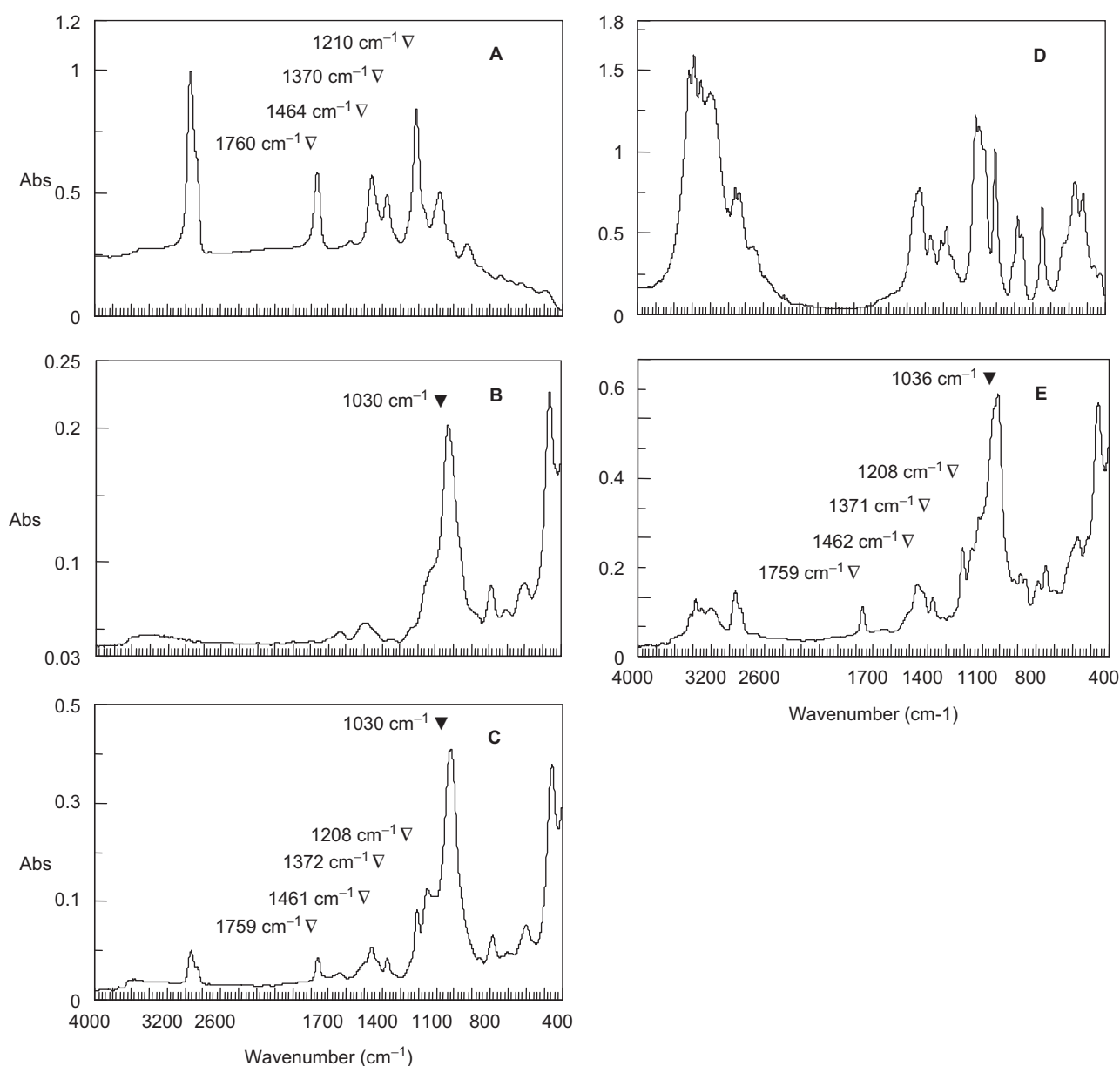


Figure 4. ATR FT-IR spectra of intact FLR, TA, xylitol, and their kneaded and physical mixtures. Key: (A) TA, (B) FLR, (C) TA/FLR, (D) xylitol, and (E) TA/FLR/xylitol.

FLR blends (Figure 4C), the peak at 1760 cm^{-1} assigned to C=O stretching and those at 1370 cm^{-1} and 1464 cm^{-1} assigned to the CH vibration mode shifted to 1759 cm^{-1} , and 1372 cm^{-1} and 1461 cm^{-1} , respectively. Moreover, the position of the peak at 1210 cm^{-1} corresponding to the C-O, -C=O and -C-O- stretching was shifted to 1208 cm^{-1} in the kneading mixture comprising TA/FLR blends (Figure 4C). In the kneading mixture comprising TA/FLR/xylitol blends (Figure 4E), the positions of the peaks at 1210 , 1370 , 1464 , and 1760 cm^{-1} corresponding to TA were shifted to 1208 , 1371 , 1462 , and 1759 cm^{-1} , respectively, which indicated the peak positions corresponding to TA in kneading mixture comprising TA/FLR blends (Figure 4C). The peaks corresponding to TA in the kneaded mixture comprising TA/FLR blends (Figure 4C) occur at the same position as those in the kneaded mixture comprising TA/FLR/xylitol blends (Figure 4E). These results suggest that TA does not interact with either FLR or xylitol.

In contrast, the positions of the peaks corresponding to FLR in the kneaded mixtures comprising TA/FLR blends were affected by kneading with xylitol (Figure 4D). The peak at 1030 cm^{-1} corresponding to intact FLR (Figure 4B) was observed in the kneaded mixtures comprising TA/FLR, but was shifted to 1036 cm^{-1} in the kneaded mixtures comprising TA/FLR/xylitol blends (Figure 4E). The sticking is eliminated by the addition of xylitol solution for kneaded mixtures comprising TA/FLR blends having TA:FLR weight ratios between 0:100 and 55:45. As shown in the previous section, the surface appearance of the kneaded mixtures comprising TA/FLR blends changed from rough to smooth due to the addition of xylitol solutions. In conjunction with the FT-IR data, this observation suggests that the change of the surface appearance of the kneaded mixtures comprising TA/FLR blends in response to the addition of xylitol may be related to interaction between xylitol and FLR.

Interaction between xylitol and FLR

As shown by the ATR FT-IR results (Figure 4), xylitol may interact with the FLR particles. To confirm the distribution states of xylitol on the FLR particles, SEM, DSC, PXRD, and ATR FT-IR analyses were carried out.

Figure 5 shows the DSC thermograms obtained during the first heating cycle of xylitol, FLR, and their kneaded and physical mixtures at approximately 75:25, 50:50, and 30:70 (w/w) ratios. During heating, the DSC curves of xylitol (100:0) exhibited a single, sharp endothermic melting peak: this occurred at 92.5°C (T_m) with an enthalpy of 182 J/g (Figure 5A), whereas that of FLR (0:100) did not exhibit an endothermic melting peak (Figure 5B). All kneaded and physical mixtures of xylitol and FLR containing 25–70% (wt/wt) FLR exhibited only one endothermic peak with a specific temperature that varied according to the xylitol/FLR ratio. The temperature and enthalpy of the peaks decreased progressively as the concentration of FLR increased from 0% to 70% (wt/wt) of FLR. The kneaded mixtures of xylitol and FLR

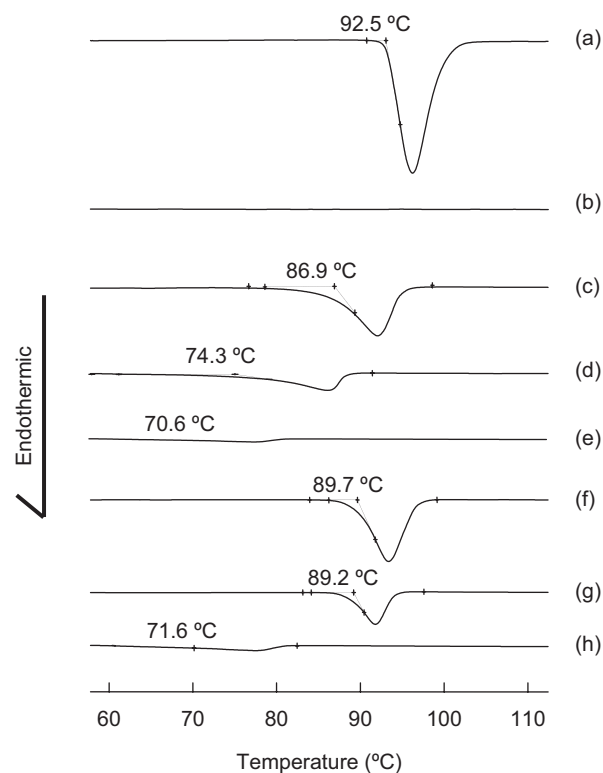


Figure 5. DSC thermograms obtained during first heating of xylitol (a) and intact FLR (b), and their kneaded (c–e) and physical (f–h) mixtures. Key: Ratio of xylitol to FLR (w/w, %) was 75:25 (c, f), 50:50 (d, g), and 30:70 (e, h).

containing 25, 50, and 70% (wt/wt) FLR exhibited endothermic peaks at 86.9°C , 74.3°C , and 70.6°C (T_m) with enthalpies of 148.0 , 84.8 , and 35.4 J/g , respectively, attributed to the melting of xylitol (Figure 5C–5E). Moreover, physical mixtures of xylitol and FLR containing 25, 50, and 70% (wt/wt) FLR exhibited endothermic peaks at 89.7°C , 89.2°C , and 71.6°C (T_m) with enthalpies of 150.0 , 84.8 , and 37.4 J/g , respectively, due to melting of xylitol (Figure 5F–5H). The thermal analysis of the kneaded and physical mixtures also suggests a possible interaction between xylitol and FLR.

Figure 6 shows SEM images of typical crystals of xylitol, FLR, and their kneaded and physical mixtures comprising xylitol/FLR blends at 50:50 (w/w). Intact FLR, which has an amorphous structure with flower-shaped particles (Figure 6B)²³, significantly affected the crystalline states of xylitol (Figure 6A), and particle aggregation between xylitol and FLR were observed in the kneaded (Figure 6C) and physical mixtures (Figure 6D) comprising xylitol/FLR blends. Moreover, the extent of aggregation between xylitol and FLR increased as the proportion of FLR increased (data not shown). As is shown in Figure 3, the surface states of the kneaded mixtures comprising TA/FLR blends changed to a smooth surface in the presence of xylitol. In addition, the representative IR bands corresponding to FLR in the kneaded mixtures comprising TA/FLR blends shifted in response to the kneading with xylitol. These results suggest that the aggregation between xylitol and FLR in the kneaded and physical

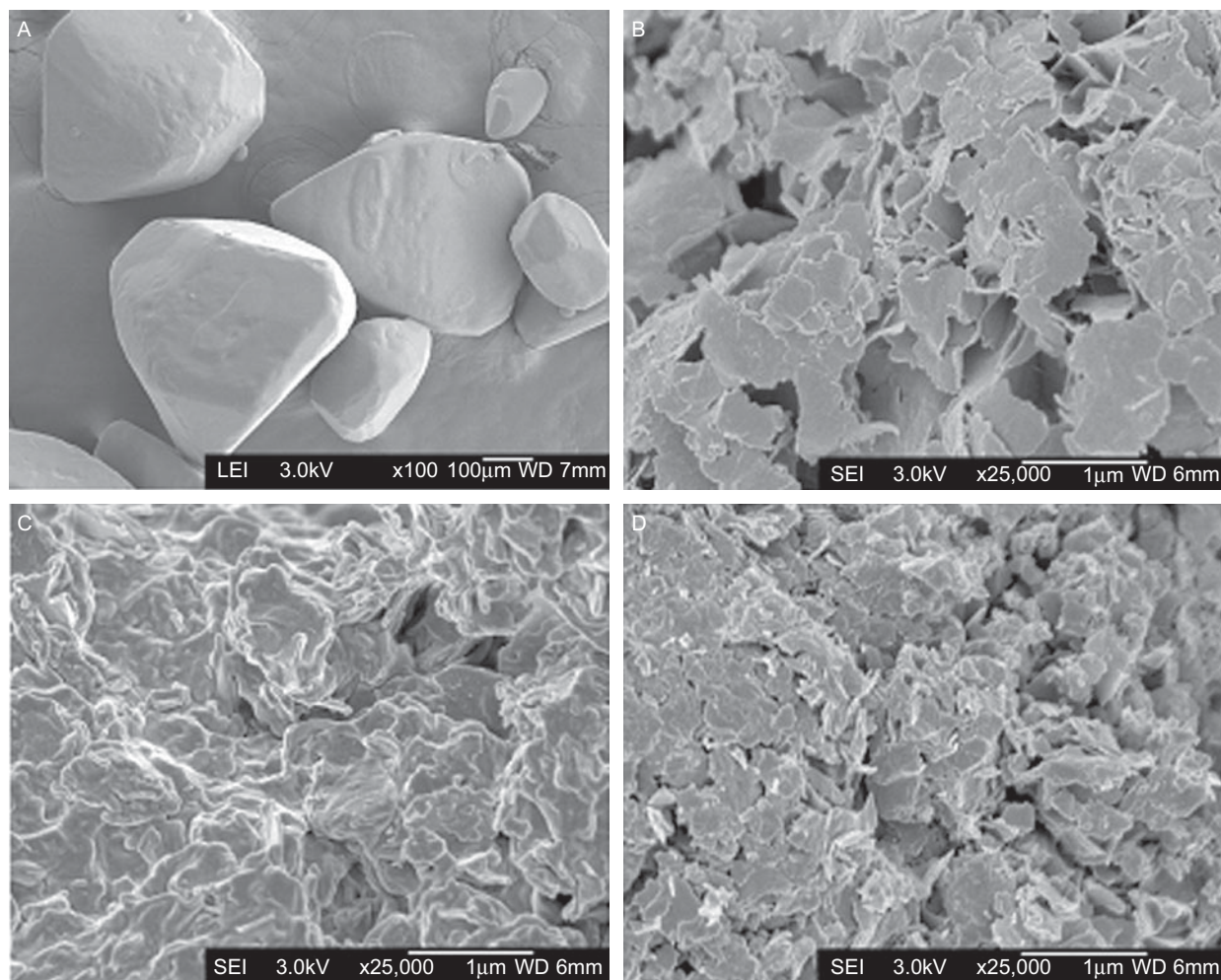


Figure 6. SEM observation of intact xylitol (A), FLR (B), and their kneaded (C) and physical (D) mixtures comprising FLR and xylitol. Key: Ratio of xylitol to FLR (w/w, %) was 50:50 (C, D).

mixtures may be related to the interaction between xylitol and FLR.

Figure 7 shows the PXRD profiles of xylitol (100:0), FLR, and their kneaded and physical mixtures at approximately 75:25, 50:50 and 30:70 (w/w) ratios. The PXRD profile of xylitol exhibited a diffraction pattern similar to that of a crystalline solid (Figure 7(a))²⁸, whereas FLR (0:100) exhibited a halo pattern similar to that of an amorphous solid (Figure 7(b)). In the kneaded mixtures comprising xylitol/FLR blends, the diffraction pattern and main diffraction angle of xylitol did not change in response to the addition of native FLR (Figure 7(c)–(e)). However, the diffraction intensity of xylitol peaks decreased considerably as compared with that of pure xylitol in response to the addition of native FLR, where the peak intensity was found to decrease with an increasing proportion of FLR (Figure 7(c)–(e)). Similarly, the PXRD intensity of xylitol in the physical mixture comprising xylitol/FLR blends decreased compared with that of pure xylitol, due to the addition of native FLR, whereas the diffraction pattern and main diffraction angle did not change (Figure 7(f)–(h)). These results suggest that the observed decrease in the intensity of the PXRD peaks of xylitol in

the presence of FLR may be related to the particle aggregation between FLR and xylitol, as shown in Figure 6. Therefore, it is reasonable to assume that the crystalline form of xylitol is readily transformed into an amorphous form in the presence of water and FLR.

Since the interaction between xylitol and FLR results in a transformation from the crystalline to amorphous form of xylitol, we studied the effect of FLR on the molecular behavior of xylitol in the kneaded and physical mixtures comprising xylitol and FLR containing 25–70% (wt/wt) FLR by using ATR FT-IR (Figure 8). The assignment of the peaks of xylitol is as follows: 3375 cm⁻¹, OH stretching vibration; 1420 cm⁻¹, CH stretching; 1065–1125 cm⁻¹, C–O, –C=O, –C–O stretching²⁹. The peak patterns in the 3000–3800 (3375 cm⁻¹) and 1065–1125 cm⁻¹ regions associated with OH and C–O, –C=O, –C–O functional groups of xylitol (Figure 8(a)) were altered significantly by addition of FLR, whereas the FT-IR spectrum of the kneaded mixture comprising xylitol/FLR shows similar patterns at various weight ratios of xylitol/FLR (Figure 8(c)–(e)). In particular, the position of the peak associated with the OH stretching vibration was observed at 3390 cm⁻¹ in the kneaded mixture comprising xylitol/FLR containing 25%

(wt/wt) FLR, at 3393 cm^{-1} in that containing 50% (wt/wt) FLR and at 3393 cm^{-1} in that containing 70% (wt/wt) FLR, respectively. The peak at 1420 cm^{-1} assigned to CH stretching shifted to 1415 cm^{-1} in the kneaded mixture comprising xylitol/FLR containing 25% (wt/wt) FLR, to 1412 cm^{-1} in that containing 50% (wt/wt) FLR and to 1412 cm^{-1} in that containing 70% (wt/wt) FLR, respectively. The peak in the $1065\text{--}1125\text{ cm}^{-1}$ region assigned to C–C, –C=O, –C–O stretching was observed at 1020 cm^{-1} in the kneaded mixtures comprising of xylitol/FLR blends containing 25–70% (wt/wt) FLR. Moreover, the peak at 1030 cm^{-1} corresponding to intact FLR (Figure 8(b)) was shifted to $1043\text{--}1048\text{ cm}^{-1}$ in the kneaded mixtures comprising xylitol/FLR blends (Figure 8(c)–(e)). The kneaded mixtures comprising xylitol/FLR blends exhibited similar IR spectra to the physical mixtures comprising xylitol/FLR blends (Figure 8(f)–(h)). The FT-IR data suggest that FLR affects the molecular behavior of xylitol in the kneaded and physical mixtures comprising xylitol/FLR blends.

It has been reported that some crystalline medicinal mixtures with adsorbents^{30–33} or porous powders^{33–36} gradually became amorphous during storage at moderate temperature. Ali et al.³⁴ reported that benzoic acid, when mixed with FLR, transformed into an amorphous ionic state within a few hours after mixing. Moreover, Ali et al.²⁴ reported that kneaded mixtures comprising FLR/flufenamic acid blends resulted in the transformation of flufenamic acid to the amorphous ionic state, predominantly to a calcium salt, and the amorphous form of the drug was found to be more stable in the mixtures having higher FLR content. As indicated by the DSC results, the melting point and heat of fusion due to melting of xylitol decreased in the presence of FLR (Figure 5). Moreover, the PXRD intensity of xylitol due to native FLR in the kneaded and physical mixtures comprising xylitol/FLR blends decreased as compared with that of pure xylitol, whereas the diffraction pattern and main diffraction angle did not change (Figure 7). These findings suggest, therefore, that the change of the molecular behavior of xylitol in response to the addition of FLR may be as a result of a possible transformation of xylitol from a crystalline form to an amorphous ionic state due to FLR particles in the kneaded and physical mixtures comprising FLR/xylitol blends; this transformation would be attributable to the interaction between FLR and xylitol.

In powder prescriptions that included kneaded mixtures comprising TA/FLR blends, the addition of xylitol effectively reduced the sticking that is typically observed in tablet compaction. In particular, the sticking caused by a tablet formulation containing TA could possibly be eliminated by combining FLR with a xylitol solution. In contrast, it was found that the sticking tended to reduce when the powder form of xylitol was physically added to the kneaded mixtures comprising TA/FLR blends as compared with the tablet formulation containing the kneaded mixtures comprising TA/FLR blends. The PXRD, DSC, and FT-IR results suggest that the powder form of xylitol may have physically interacted with FLR in the

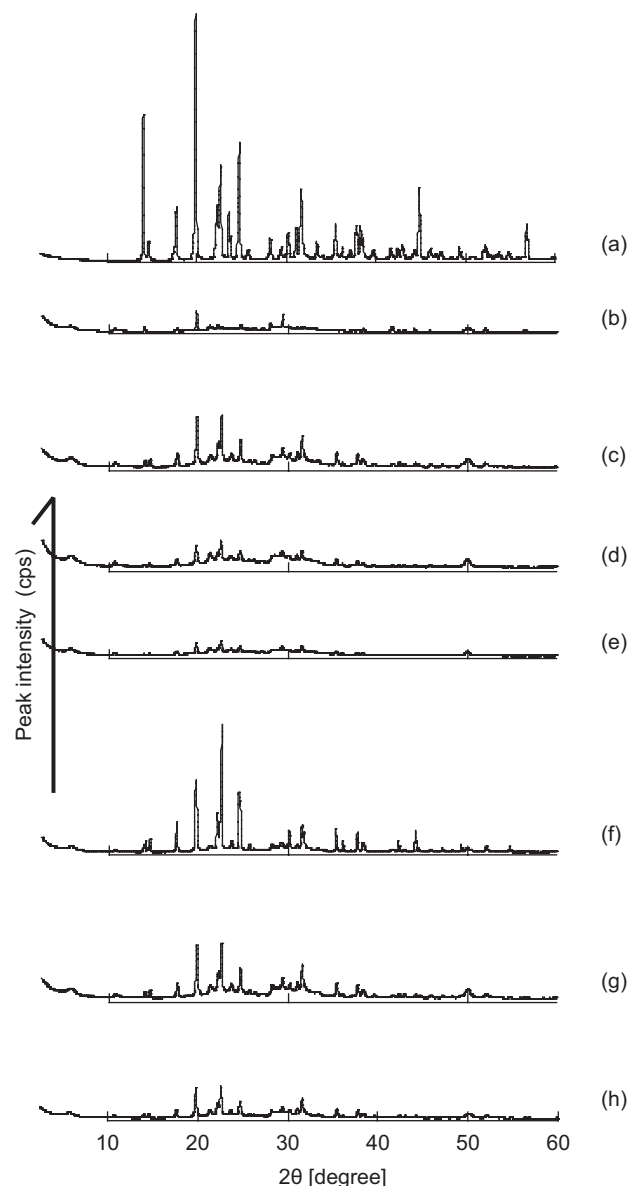


Figure 7. PXRD of xylitol (a), intact FLR (b), and their kneaded (c–e) and physical (f–h) mixtures. Key: Ratio of xylitol to FLR (w/w, %) was 75:25 (c, f), 50:50 (d, g), 30:70 (e, h).

same manner as in the kneaded mixtures comprising FLR/xylitol blends. The physical mixtures comprising xylitol/FLR blends exhibited IR spectra that were similar to those of the kneaded mixtures comprising xylitol/FLR blends. However, it is also worth noting that the PXRD pattern of the kneaded mixture had a lower peak intensity than that of the physical mixture. As indicated by the DSC results, the melting point and heat of fusion because of the melting of xylitol in the kneaded mixture were lower than those in the physical mixture. Since the interaction between FLR and xylitol occurred more readily in the solution form of xylitol than in its powder form, the occurrence of sticking may be dependent on the distribution states of xylitol on FLR in a mixture comprising a TA/FLR/xylitol blend. It is well-known that FLR has many interparticle and intraparticle pores on its surface, particularly those with a size of 12 and $0.15\text{ }\mu\text{m}$,

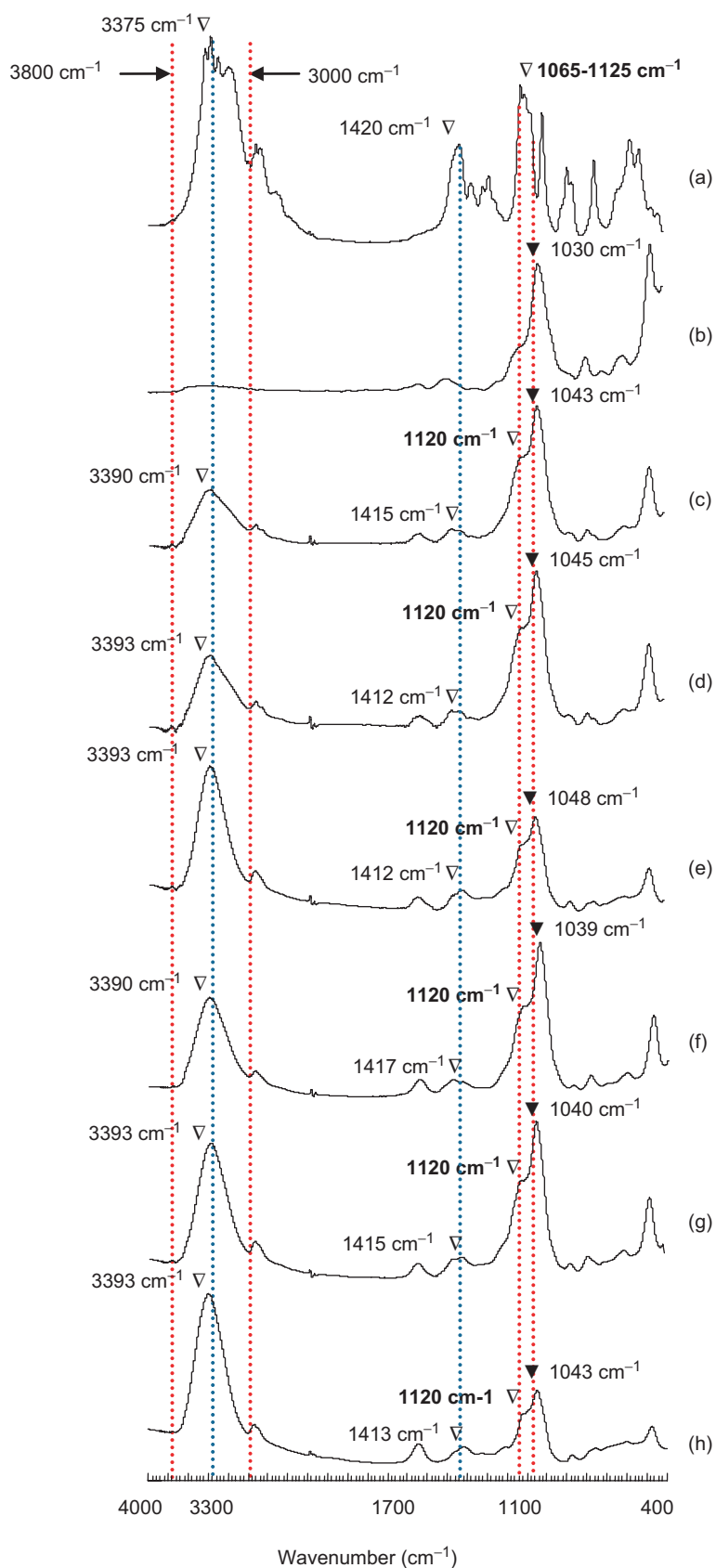


Figure 8. ATR FT-IR spectra of xylitol (a), intact FLR (b), and their kneaded (c-e) and physical (f-h) mixtures. Key: Ratio of xylitol to FLR (w/w, %) was 75:25 (c, f), 50:50 (d, g), 30:70 (e, h).

respectively. The surface areas of the kneaded mixtures comprising TA/FLR blends decreased sharply by the addition of xylitol solutions, which suggests that xylitol was distributed in the interparticle and intraparticle pores of FLR in the kneaded mixtures comprising the TA/FLR/xylitol blends. In addition, the effect of the powder form of xylitol on the surface areas of the kneaded mixtures comprising TA/FLR blends was investigated. In the presence of the powder form of xylitol, the kneaded mixtures of FLR and TA containing 33%, 50%, and 55% (wt/wt) TA had surface areas of 74.5, 51.4, and 33.5 m²/g, respectively. However, the decreases in the surface areas of the TA/FLR blends caused by the powder form of xylitol were lower than those caused by the xylitol solutions. Moreover, the physical mixtures comprising FLR/xylitol blends exhibited rough surfaces as compared with the kneaded mixtures comprising FLR/xylitol blends, which exhibited smooth surfaces because of the interaction between xylitol and FLR. These results suggest that the distribution states of xylitol on the interparticle and intraparticle pores of FLR in the kneaded mixtures comprising TA/FLR/xylitol blends were different between the xylitol solution and the powder form of xylitol. It is well-known that the occurrence of sticking depends on the characteristics and surface condition of particles. Therefore, these results suggest that the occurrence of sticking can be prevented not only by the inhibition of TA evolution from the interparticle and intraparticle pores of FLR but also by controlling the surface conditions of the TA particles arising as a result of the interaction between FLR and xylitol in kneaded mixtures comprising TA/FLR/xylitol blends.

Conclusions

We found that the addition of xylitol to an FLR powder formulation containing TA effectively decreased the sticking that is typically observed during tablet compaction. Sticking was eliminated by the addition of a xylitol solution to kneaded mixtures comprising TA/FLR blends. In contrast, sticking could not be completely eliminated when the powder form of xylitol was physically added to the kneaded mixtures comprising TA/FLR blends. In an attempt to clarify the relationship between the distribution states of xylitol on the FLR particles and the occurrence of sticking, nitrogen gas adsorption, SEM, DSC, PXRD, and ATR FT-IR analyses were carried out. The nitrogen gas adsorption analysis indicated that xylitol may have been distributed on the interparticle and intraparticle pores of FLR in the kneaded and physical mixtures comprising TA/FLR/xylitol blends. Moreover, the analyses results indicate that xylitol may have interacted with FLR in the physical and kneaded mixtures comprising FLR/xylitol blends. However, the interaction between FLR and xylitol occurred more readily in the kneaded mixtures comprising FLR/xylitol blends than in the physical mixtures comprising FLR/xylitol blends. It is well-known that sticking occurs during

tablet compaction when particles of a tablet formulation comprising an oily medicine and excipients adhere to the punch face. The kneaded mixtures comprising FLR/xylitol blends had smooth surfaces as compared with the physical mixtures comprising FLR/xylitol blends. In addition, we observed that the kneaded mixtures comprising TA/FLR blends changed from a rough surface to a smooth one on kneading with xylitol, which showed a smooth surface as compared with the physical mixtures comprising TA/FLR/xylitol blends. Therefore, the distribution states of xylitol on FLR particles may be related to the occurrence of sticking. The results of this study indicate that the occurrence of sticking can be eliminated during tablet compaction by inhibiting the TA evolution from the interparticle and intraparticle pores of FLR as a result of the interaction between FLR and xylitol in kneaded mixtures comprising TA/FLR/xylitol blends. The results of this study provide basic information that is pertinent to the formulation and manufacturing process of a tablet containing an oily medicine.

Declaration of interest

The authors report no declarations of interest.

References

1. Takeuchi H, Sasaki H, Niwa T, Hino T, Kawashima Y, Uesugi K et al. (1991). Redispersible dry emulsion system as novel oral dosage form of oily drugs: *in vivo* studies in beagle dogs. *Chem Pharm Bull*, 39:3362–3364.
2. Kimura T, Fukui E, Kageyu A, Kurohara H, Kurosaki Y, Nakayama T et al. (1989). Enhancement of oral bioavailability of D-alpha-tocopherol acetate by lecithin-dispersed aqueous preparation containing medium-chain triglycerides in rats. *Chem Pharm Bull*, 37:439–441.
3. Takeuchi H, Sasaki H, Niwa T, Hino T, Kawashima Y, Uesugi K et al. (1992). Design of redispersible dry emulsion as an advanced dosage form of oily drug (vitamin E nicotinate) by spray-drying technique. *Drug Dev Ind Pharm*, 18:919–937.
4. James S, James CB. (2002). *Encyclopedia of Pharmaceutical Technology*, 2nd ed. Marcel Dekker, New York, p. 2669.
5. Schmidt Von PC, Stefens KJ, Kneble G. (1983). Vereinfachung der registrierung physikalischer parameter bei der tablettierung. *Pharm Ind*, 45:800–805.
6. Naito SI, Nakamichi K. (1969). Studies on techniques of manufacturing pharmacy. I. Prediction of tableting troubles such as capping and sticking. 1. *Chem Pharm Bull*, 17:2507–2514.
7. Naito S, Shimizu I, Iwaki S. (1971). Techniques for manufacturing pharmacy. II. Prediction of tableting troubles such as capping and sticking. 2. *Chem Pharm Bull*, 19:1949–1956.
8. Naito SI, Masui K, Shiraki T. (1977). Prediction of tableting problems such as capping and sticking: theoretical calculations. *J Pharm Sci*, 66:254–259.
9. Toyoshima K, Yasumura M, Onishi N, Ueda Y. (1988). Quantitative evaluation of tablet sticking by surface roughness measurement. *Int J Pharm*, 46:211–215.
10. Danjo K, Kojima S, Chen CY, Sunada H, Otsuka A. (1997). Effect of water content on sticking during compression. *Chem Pharm Bull*, 45:706–709.
11. Kinoshita M, Baba K, Nagayasu A, Yamabe K, Shimooka T, Takeichi Y et al. (2002). Improvement of solubility and oral bioavailability of a poorly water-soluble drug, TAS-301, by its melt-adsorption on a porous calcium silicate. *J Pharm Sci*, 91:362–370.

12. Oguchi T, Tozuka Y, Okunogi S, Yonemochi E, Yamamoto K. (1997). Improved dissolution of naproxen from solid dispersions with porous additives. *J Pharm Sci Technol Jpn*, 57:168-173.
13. Takeuchi H, Nagira S, Yamamoto H, Kawashima Y. (2004). Solid dispersion particles of tolbutamide prepared with fine silica particles by the spray-drying method. *Powder Tech*, 141:187-195.
14. Takeuchi H, Nagira S, Yamamoto H, Kawashima Y. (2005). Solid dispersion particles of amorphous indomethacin with fine porous silica particles by using spray-drying method. *Int J Pharm*, 288:177-183.
15. Gupta MK, Vanwert A, Bogner RH. (2003). Formation of physically stable amorphous drugs by milling with Neusilin. *J Pharm Sci*, 92:536-551.
16. Byrne RS, Deasy PB. (2002). Use of commercial porous ceramic particles for sustained drug delivery. *Int J Pharm*, 246:61-73.
17. Ito Y, Arai H, Uchino K, Iwasaki K, Shibata N, Takada K. (2005). Effect of adsorbents on the absorption of lansoprazole with surfactant. *Int J Pharm*, 289:69-77.
18. Jain SK, Agrawal GP, Jain NK. (2007). Porous carrier based floating granular delivery system of repaglinide. *Drug Dev Ind Pharm*, 37:381-391.
19. Streubel A, Siepmann J, Bodmeier R. (2002). Floating microparticles based on low density foam powder. *Int J Pharm*, 241:279-292.
20. Streubel A, Siepmann J, Bodmeier R. (2003). Floating matrix tablets based on low density foam powder: effects of formulation and processing parameters on drug release. *Eur J Pharm Sci*, 18:37-45.
21. Yuasa H, Takashima Y, Kanaya Y. (1996). Studies on the development of intragastric floating and sustained release preparation. I. Application of calcium silicate as a floating carrier. *Chem Pharm Bull*, 44:1361-1366.
22. Yuasa H, Akutagawa M, Hashizume T, Kanaya Y. (1996). Studies on internal structure of tablets. VI. Stress dispersion in tablets by excipients. *Chem Pharm Bull*, 44:378-382.
23. Yuasa H, Asahi D, Takashima Y, Kanaya Y, Shinozawa K. (1994). Application of calcium silicate for medicinal preparation. I. Solid preparation adsorbing an oily medicine to calcium silicate. *Chem Pharm Bull*, 42:2327-2331.
24. Ali AS, Yamamoto K, El-sayed AM, Habib FS, Nakai Y. (1992). Molecular behavior of flufenamic acid in physical and ground mixtures with fluorite. *Chem Pharm Bull*, 40:1289-1294.
25. Ekgasit S, Pattayakorn N, Tongsakul D, Thammacharoen C, Kongyot T. (2007). A novel ATR FT-IR microspectroscopy technique for surface contamination analysis without interference of the substrate. *Anal Sci*, 23:863-868.
26. Planinsek O, Planinsek D, Zega A, Breznik M, Srcic S. (2006). Surface analysis of powder binary mixtures with ATR FTIR spectroscopy. *Int J Pharm*, 319:13-19.
27. Tocopherol acetate monograph in JP XV, p. C-2705-9.
28. Madsen AØ, Sørensen HO, Flensburg C, Stewart RF, Larsen S. (2004). Modeling of the nuclear parameters for H atoms in X-ray charge-density studies. *Acta Crystallogr, A, Found Crystallogr*, 60:550-561.
29. Xylitol monograph in JP XV, p. C-1040-5.
30. Kim KH, Frank MJ, Henderson NL. (1985). Application of differential scanning calorimetry to the study of solid drug dispersions. *J Pharm Sci*, 74:283-289.
31. Konno T, Kinuno K, Kataoka K. (1986). Physical and chemical changes of medicinals in mixtures with adsorbents in the solid state. I. Effect of vapor pressure of the medicinals on changes in crystalline properties. *Chem Pharm Bull*, 34:301-307.
32. Konno T, Kinuno K. (1989). Physical and chemical changes of medicinals in mixtures with adsorbents in the solid state. II. Application of reduced pressure treatment for the improvement of dissolution of flufenamic acid. *Chem Pharm Bull*, 37:2481-2484.
33. Nakai Y, Yamamoto K, Terada K, Oguchi T, Yamamoto M. (1987). [Study of the interaction between light anhydrous silicic acid and drugs]. *Yakugaku Zasshi*, 107:294-300.
34. Ali AS, Yamamoto K, El-sayed AM, Habib FS, Nakai Y. (1992). Molecular interaction between benzoic acid and fluorite and complex formation. *Chem Pharm Bull*, 40:467-471.
35. Nakai Y, Yamamoto K, Terada K, Ichikawa J. (1984). Interaction of medicinals and porous powder. I. Anomalous thermal behavior of porous glass mixtures. *Chem Pharm Bull*, 32:4566-4571.
36. Nakai Y, Yamamoto K, Terada K, Oguchi T, Izumikawa S. (1986). Interactions between crystalline medicinals and porous clay. *Chem Pharm Bull*, 34:4760-4766.